Korean J. Chem. Eng., **25**(2), 223-230 (2008)

High temperature desulfurization over nano-scale high surface area ceria for application in SOFC

Rajesh Shivanahalli Kempegowda, Navadol Laosiripojana† and Suttichai Assabumrungrat*

The Joint Graduate School of Energy and Environment, King Mongkut's University of Technology Thonburi, Bangkok 10140, Thailand
*Center of Excellence in Catalysis and Catalytic Reaction Engineering, Department of Chemical Engineering, Faculty of Engineering, Chulalongkorn University, Bangkok 10330, Thailand
(*Received 13 February 2007 • accepted 27 July 2007*)

Abstract−In the present work, suitable absorbent material for high temperature desulfurization was investigated in order to apply internally in solid oxide fuel cells (SOFC). It was found that nano-scale high surface area CeO_2 has useful desulfurization activity and enables efficient removal of H_2S from feed gas between 500 to 850 °C. In this range of temperature, compared to the conventional low surface area CeO_2, 80-85% of H_2S was removed by nano-scale high surface area CeO_2, whereas only 30-32% of H_2S was removed by conventional low surface area CeO_2. According to the XRD studies, the product formed after desulfurization over nano-scale high surface area CeO_2 was Ce_2O_2S. EDS mapping also suggested the uniform distribution of sulfur on the surface of CeO_2. Regeneration experiments were then conducted by temperature programmed oxidation (TPO) experiment. Ce_2O_2S can be recovered to CeO_2 after exposure in the oxidation condition at temperature above 600 °C. It should be noted that SO_2 is the product from this regeneration process. According to the SEM/EDS and XRD measurements, all Ce_2O_2S forming is converted to CeO_2 after oxidative regeneration. As the final step, a deactivation model considering the concentration and temperature dependencies on the desulfurization activity of CeO_2 was applied and the experimental results were fitted in this model for later application in the SOFC model.

Key words: Desulfurization, SOFC, CeO_2, Deactivation Model

INTRODUCTION

Due to the present oil crisis and global warming, numerous efforts have been focused on the use of alternative and renewable energy sources. Biogas is one important energy source due to its closed cycle operation and producibility from biodegradable solid wastes such as cattle dung (diary wastes), piggery wastes, municipal solid wastes, and industrial effluents. Currently, there are numerous attempts to use biogas as a primary fuel for electrical generation by using several energy devices, i.e., internal combustion engines and fuel cells. As biogas always contains high concentration of hydrogen sulfide (H_2S) (approximately 1,000-2,000 ppm depending on its source), it cannot be utilized directly to the energy devices. Biogas must be initially purified in order to remove H_2S which easily poisons the process reactor. In addition, the removal of H_2S would also help in preventing odors, safety hazards, and corrosion of the biogas transport equipment.

The appropriate technologies of desulfurization depend on the final applications as well as the operating conditions. Several researchers have studied desulfurization by selective oxidation of H_2S over solid absorbents at low temperature (200-300 °C). Park et al. [1] investigated this reaction over $Bi_4V_{2-x}Sb_xO_{11-y}$ material and reported good H_2S conversion with less than 2% of SO_2 selectivity in the temperature range of 220-260 °C. Lee et al. [2] also studied this desulfurization reaction on zeolite-NaX and zeolite-KX. They found that Zeolite-KX was superior to the zeolite-NaX in terms of selectivity to elemental sulfur and resistance to deactivation. In detail, elemental sulfur yield over zeolite-NaX was achieved at about 90% at 225 °C for the first 4 hours, but gradually decreased to 55% after 40 hours, whereas the yield of elemental sulfur on zeolite-KX was obtained within the range of 86% at 250 °C after 40 hours.

It should be noted that selective oxidation may not suitable for high temperature applications such as coal or residual oil gasification, and fuel cell applications, which operate in the temperature range of 400-1,200 °C, due to the large temperature differences in the process. Several high temperature desulfurization techniques are, therefore, desired for use in such applications [3]. Previously, the high temperature removal of hydrogen sulfide from simulated gas was carried out in batch type fluidized-bed reactor by using natural manganese ore consisting of several metal oxides (MnO_x: 51.85%, FeO_y: 3.86%, CaO: 0.11%) [4]. It was found that H_2S removal efficiency increased with increasing temperature but decreased with increasing excess gas velocity. In addition, the breakthrough time for H_2S decreased as the gas velocity increased.

As another example of the high temperature application, fuel cell has drawn a great interest from many researchers as it can generate electricity at high efficiency. Various types of fuel cells are available, in that the solid oxide fuel cell (SOFC) has garnered much attention because of its large electricity production capacity. To establish these highly efficient processes, it is necessary to develop a high temperature treatment process for the various feed stocks, i.e., biogas and natural gas, which consist of a significant amount of H_2S. To date, fuel cell systems rely mainly on batch operation of sorbent

†To whom correspondence should be addressed.
E-mail: navadol_l@jgsee.kmutt.ac.th

technology for sulfur removal. Although this technology possesses the necessary removal efficiency, the low capacity associated with the batchwise operation and the potential utilization of high sulfur hydrocarbon feed stocks greatly affect the fuel cell processor foot print, types of sorbent and sorbent maintenance interval [5]. A widely established metal oxide, ZnO, has been used as a high temperature desulfurization sorbent. ZnO has the most favorable thermodynamics for H_2S removal among sorbents that have been investigated. However, despite its attractive thermodynamic properties, the reduction of ZnO and subsequent vaporization of elemental zinc create a serious problem over many cycles of sulfidation/regeneration at high temperatures [6,7]. As a result, alternate absorbents to minimize ZnO problems at high temperature ranges are needed.

Meng et al. [8] and Kay et al. [9] first described the use of cerium oxide (or ceria) sorbents for high-temperature desulfurization. It is well established that ceria and metal oxide (e.g., Gd, Nb, and Zr) doped cerias provide high oxygen storage capacity, which is beneficial in oxidation processes. Several researchers have also reported the benefit of adding or doping this material on the reforming and partial oxidation catalysts in terms of catalyst stability and the resistance toward carbon deposition [10,11]. Focusing on the use of ceria as the sorbent for desulfurization, in laboratory-scaled fixed-bed reactor tests, the H_2S concentration was reduced from 1.2 v% to 3 ppmv at 872 °C and 1 atm by using reduced ceria, CeO_n ($n<2$). However, only a few data were reported particularly on the material characterization and the mechanism of desulfurization. Abbasian et al. [12] and Li et al. [13] studied mixed-oxide sorbents containing cerium and copper oxides. Although some evidence of cerium sulfidation was reported, the primary function of the ceria was considered to be for maintaining the active copper in a highly dispersed form. Zeng et al. [14] studied the H_2S removal in presence of hydrogen on CeO_2 sorbent. They reported complete conversion of CeO_2 to CeO_2S during sulfidation in the temperature range of 500-700 °C and regeneration of Ce_2O_2S to CeO_2 by using SO_2. According to phase diagrams, relevant reactions were reported by Kay et al. [9] as:

Sulfidation

$$2CeO_2+H_2S+H_2 \leftrightarrow Ce_2O_2S+2H_2O \quad (1)$$

Regeneration

$$Ce_2O_2S+SO_2 \leftrightarrow 2CeO_2+S_2 \quad (2)$$

It should be noted that the major limitations to apply CeO_2 in the high temperature process are its low specific surface and high surface area reduction percentage due to the high surface sintering. It was observed from our previous work that the surface area reduction of CeO_2 after exposure in the reaction conditions at 900 °C was 23% and 28%, respectively. The corresponding post-reaction specific surface areas were only 1.9 and 8.7 $m^2\ g^{-1}$, respectively [15]. The use of high surface area CeO_2 would be a good alternative procedure to improve the performance of H_2S removal at high temperature. In this paper, nano-scale high surface area CeO_2 (from nano-Arc Company, US) was used as a sorbent for the desulfurization process. The reactions during sulfidation and oxidative regeneration were investigated. Some analytical techniques were employed to characterize the sorbents at different stages of operation. In addition, the deactivation model considering the concentration dependency of the activity was developed and fitted with the experimental results to determine the kinetic parameters for the later application in SOFC model fueled by conventional fuel: biogas and natural gas. Regarding the selection of the suitable model, it should be noted that the formation of a dense product layer over the solid reactant results in an additional diffusion resistance and is expected to cause a drop in the reaction rate. One would also expect it to cause significant changes in the pore structure, active surface area, and activity per unit area of solid reactant with reaction extent. These changes cause a decrease of the solid reactant activity with time. As reported in the literature, the deactivation model works well for such gas-solid reactions [16]. In this model, the effects of these factors on the diminishing rate of sulfur fixation were combined in a deactivation rate term [17].

EXPERIMENTAL

1. Fixed Bed Reactor Setup

A laboratory-scaled fixed bed quartz reactor of 30 cm height and 0.635 cm internal diameter was installed vertically in an electric furnace with a programmable temperature controller. Nano-scale CeO_2 (from nano-Arc Company, US) was first calcined at 900 °C before packing between two layers of quartz wool. The physical and chemical properties of CeO_2 are provided in Table 1. A type K thermocouple was located externally at the center of the catalyst to monitor the temperature of the reactor. Swagelok fittings and tubing were used to connect the reactor to the gas supply and gas sampling systems. Details of the reactor setup were shown in Fig. 1.

2. Analytical Methods

Pure CeO_2 and spent CeO_2 were characterized by using X-ray diffractometer (XRD) employing Cu 30 kW and 15 mA to determine the sulfur deposition on the sorbent. SEM and EDS analysis was also carried out to investigate the changes in morphology and sulfur distribution by elemental mapping. The conditions used were 40 kV and resolution of 4000.

Table 1. Physical and chemical properties of CeO_2

Surface area (m^2g^{-1})	42.819
Bulk density	9.102
Pore volume	9.7443×10^{-2}

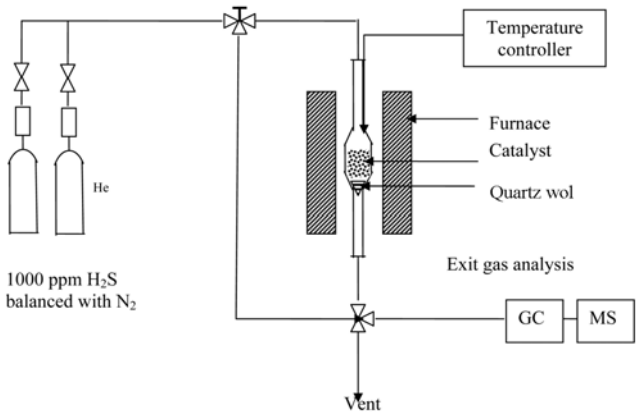

Fig. 1. Schematic diagram of experimental setup.

Table 2. Operating conditions of GC

Detector	TCD
Detector temperature (°C)	150
Column	Porapak-Q
Oven temperature (°C)	Linear programming @ 20 °C min^{-1}
Current (mA)	150

3. Gas Analysis

Gas analysis was carried out by using Shimadzu gas chromatography (GC-14B) equipped with a Porapak-Q column and a TCD detector. The H_2S peak was obtained by using a linear temperature programming in the column oven. The temperature was increased from 40 to 200 °C at a ramp rate of 20 °C min^{-1}. The operating conditions of the GC are summarized in Table 2. It should be noted that the TCD calibration was carried out by mixing pure H_2S and N_2 at various ratios. Mixture of 0.01% (molar) H_2S balanced with nitrogen was used to calibrate the concentration by diluting with helium gas.

4. Procedures for Sulfidation Experiments

The sulfidation experiments were carried out in a fixed bed reactor. The experimental procedures were divided into the study of optimum temperature and the establishment of breakthrough curves for the adsorption of H_2S on CeO_2 sorbent.

Regarding the study of optimum temperature, a set of experiments was carried out to test the desulfurization activity of CeO_2 sorbent at various temperatures: 400, 500, 600, 700, 800 and 850 °C. The amount of CeO_2 was kept at 500 mg, while the total flow rate was 100 cm^3 min^{-1}. The temperature was increased linearly at a rate of 10 °C min^{-1} until reaching a desired temperature. The reactor was then kept under isothermal condition for 30 min. The exit gases from the reactor were connected to the gas chromatography (GC) equipped with TCD detector to detect the H_2S level after adsorption at each temperature level. The breakthrough curve experiments were then carried out at the suitable temperatures for the desulfurization. The reactor was operated by using a feed gas (100 cm^3 min^{-1}) with H_2S concentration of 1,000 ppm. The reactor was heated to a desired temperature at a heating rate of 10 °C min^{-1}. The system was operated under isothermal until breakthrough of H_2S appeared at the exit of the bed.

5. Oxidative Regeneration of Sulfided CeO_2 by Temperature Programmed Reaction Study

The characteristics of the regeneration of the sulfided CeO_2 were examined with a temperature programmed oxidation (TPO) apparatus equipped with quadrupole mass spectrometer. In the TPO examination, 10% oxygen balanced in helium or nitrogen was fed into the microreactor in the TPO apparatus at a flow rate of 100 cm^3 min^{-1}. A sample of 50 mg was packed into the micro reactor of ¼" size. The sample was heated to 900 °C at a constant heating rate of 10 °C min^{-1}. The exit gases were monitored continuously with the mass spectrometer.

RESULTS AND DISCUSSION

1. Sulfidation Results

First, the effect of temperature on the desulfurization activity of nano-scale CeO_2 sorbent was studied in the range of 400 to 850 °C.

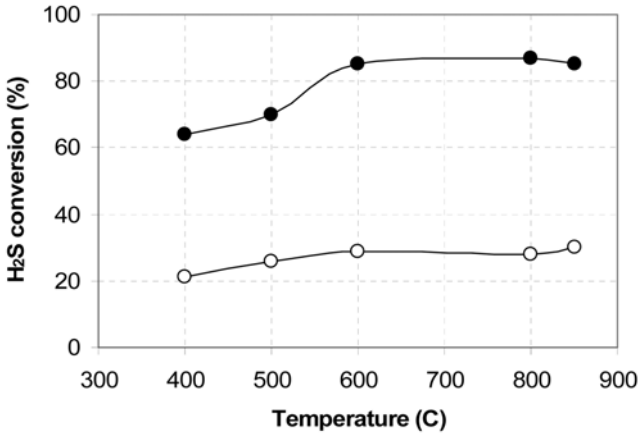

Fig. 2. Conversions of H_2S at different temperatures (nano-scale high surface area CeO_2 (●), and conventional low surface area CeO_2 (○)).

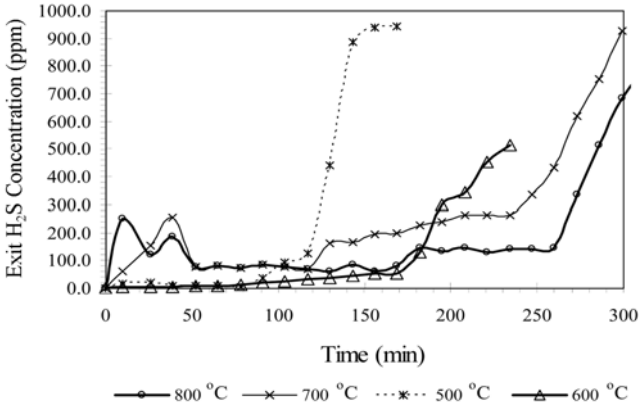

Fig. 3. Sulfidation break through curves of CeO_2.

The conversion of H_2S (X) defined in Eq. (3) was plotted with temperature as shown in Fig. 2. It should be noted that the desulfurization activity of conventional low surface area CeO_2 (synthesized by the precipitation method with the specific surface area of 3.1 m^2 g^{-1}) was also performed for comparison.

$$X = \frac{Conc_{Initial} - Conc_{Exit}}{Conc_{Initial}} \times 100 \quad (3)$$

It was found that the H_2S conversion from the desulfurization over nano-scale CeO_2 was almost 3 times higher than that over conventional low surface area CeO_2. The conversion increased readily with increasing temperature and then became constant at above 600 °C. The breakthrough results for nano-scale CeO_2, which refers to a predetermined H_2S outlet condition when a certain concentration of H_2S cannot be removed by the catalyst bed [18], at several temperatures are presented in Fig. 3. As seen from the figure, the breakthrough period increased with increasing temperature. It should be noted that a few bumps (higher H_2S concentration regions) appeared in some early part of the pre-breakthrough curves. These early bumps could be associated with incomplete reduction of ceria at the early state. Without pre-reduction, the reduction and sulfidation occurred simultaneously on the surface of ceria, as explained by Zeng et al.

[14]. According to the gas product detected from gas chromatography during the sulfidation testing, small amounts of hydrogen and oxygen were also detected along with steam, which could have been formed by the combustion of hydrogen and oxygen.

2. Regeneration of Sulfided CeO_2

Regeneration of sulfided CeO_2 was conducted by using 10% oxygen as a regeneration agent for two different samples sulfided at 700 and 800 °C. A sample was packed and heated in a micro tube reactor installed in the furnace at a constant heating rate of 10 °C min^{-1}. The amount of O_2 and SO_2 evolved at each temperature level was monitored by mass spectrometer. Figs. 4 and 5 show the results of the samples sulfided at 700 and 800 °C, respectively. Both figures indicate the consumption of O_2 and evolution of SO_2 during the temperature range of 600 and 800 °C. The evolution temperature observed in the present work is in good agreement with several previous works in the literature [19-21], which investigated the oxidation of Ce_2O_2S in the range of operating temperature between 600-800 °C by TPO technique and observed the evolution of SO_2 around 800 °C. According to the calculation of area under peaks from Figs. 4 and 5, the amount of SO_2 evolved was approximately 1.25 mol% from the sulfided sample at 700 °C by consuming oxygen of 2% whereas the amount of SO_2 evolved from the sulfided sample at 800 °C was about 3 mol% with the oxygen consuming of 4%. The difference in the amount of SO_2 evolution from the sulfidation at different temperatures, which was also observed by several researchers, could be mainly due to the increase of oxygen mobility on the

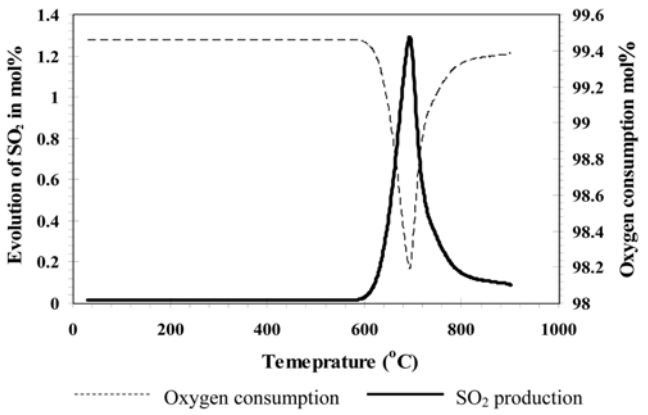

Fig. 4. Oxidative regeneration of CeO_2 sulfided at 700 °C.

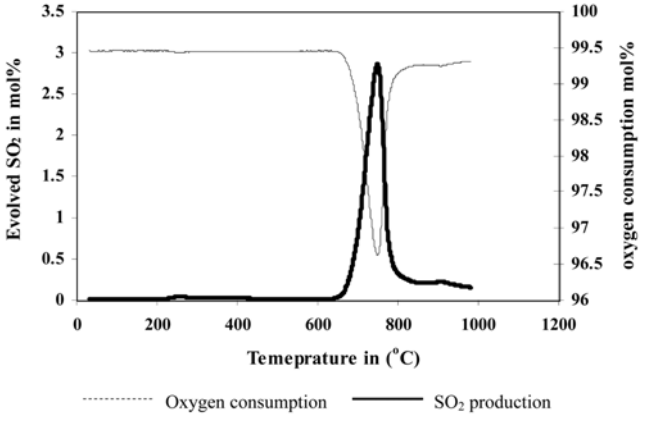

Fig. 5. Oxidative regeneration of CeO_2 sulfided at 800 °C.

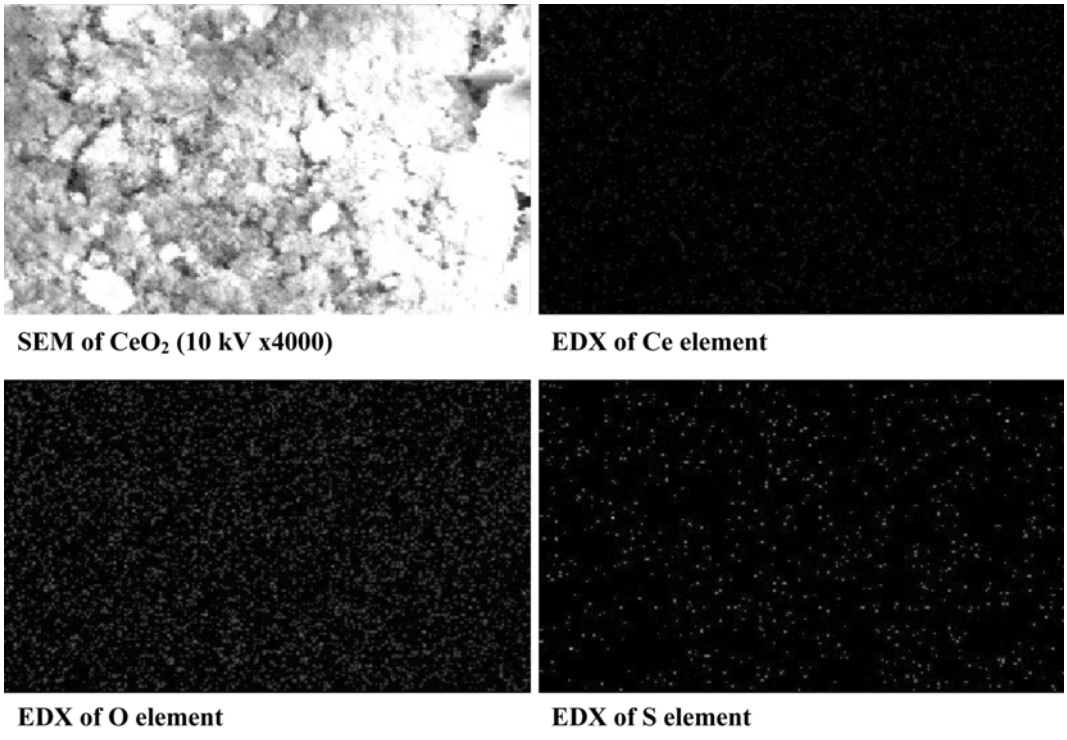

(a) SEM and elemental mapping of CeO_2 sulfided at 700°C

Fig. 6. Mapping of sulfur, oxygen and cerium distribution on the sulfided CeO_2.

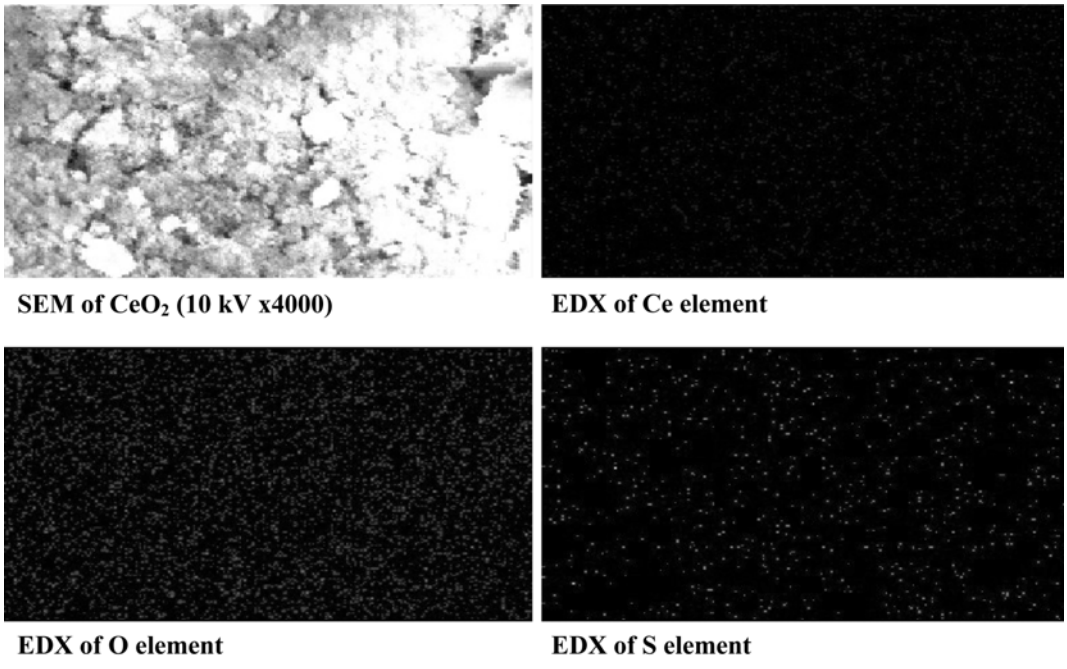

(b) SEM and elemental mapping of CeO_2 sulfided at 800°C

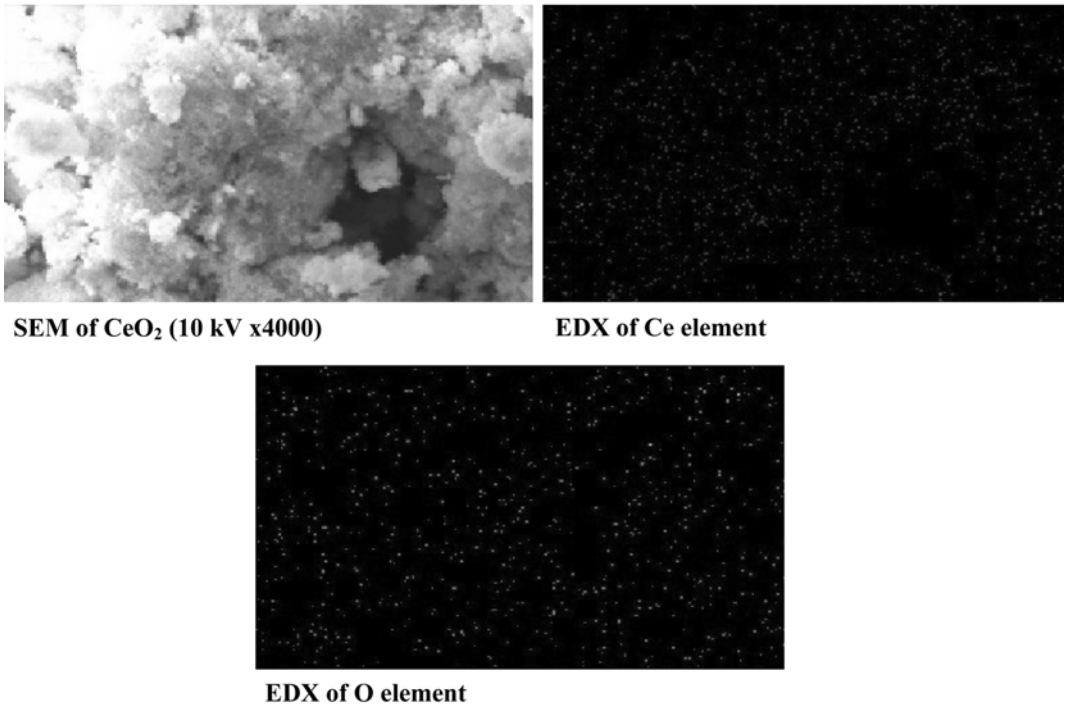

(c) SEM and elemental mapping of regenerated CeO_2

Fig. 6. Continued.

surface of CeO_2 by increasing temperature. It is well established that ceria-based material contains a high concentration of highly mobile oxygen vacancies, which act as local sources or sinks for oxygen involved in reactions taking place on its surface. That high oxygen mobility, high oxygen storage capacity, and its modifiable ability render the ceria-based material very interesting for a wide range of catalytic applications. At higher temperature, the gas-solid reaction between the inlet sulfur compound and the bulk lattice oxygen on the surface of CeO_2 occurred easily, and consequently resulted in a high sulfidation reaction [22]. Previous work from Zeng et al. [14] also reported that the degree of sulfidation increases with increasing temperature.

3. Characterization of Absorbent

Sulfided CeO_2 was subjected to its surface analysis by SEM/EDS and XRD measurements to determine the distribution of sulfur and the type of product formation on the surface of the CeO_2. From the SEM & EDS mapping as shown in Fig. 6, sulfur distribution on the surface of the catalyst was detected. According to the sulfur distribution at 700 and 800 °C, as shown in Figs. 6(a) and 6(b), respectively, the sulfur concentrations at 800 °C are higher than those at 700°C, which is in good agreement with the observed SO_2 peaks shown in Figs. 4 and 5. In addition, from the sulfur mapping observed by the EDS, it was found that the sulfur element was uniformly distributed over the surface of CeO_2. Larger particles in the figure are due to aggregation of smaller particles and the change in the porous structure. As CeO_2 consists of high surface oxygen ions, these ions make it become easily exchanged to sulfur upon H_2S adsorption [23].

In addition to the SEM/EDS measurement, sulfided CeO_2 was subjected to XRD studies to determine the type product formed. From the XRD analysis as shown in Fig. 8, major phases of the sulfided CeO_2 are Ce_2O_2S (Pattern 26-1085). The pattern was compared with that of pure CeO_2 (pattern 34-0394) as shown in Fig. 7. The XRD patterns of spent CeO_2 indicate that the cerium oxide sulfide (Ce_2O_2S) was formed from the reaction of CeO_2 with H_2S. Peaks of spent CeO_2 were decreased and peak broadening occurred at the

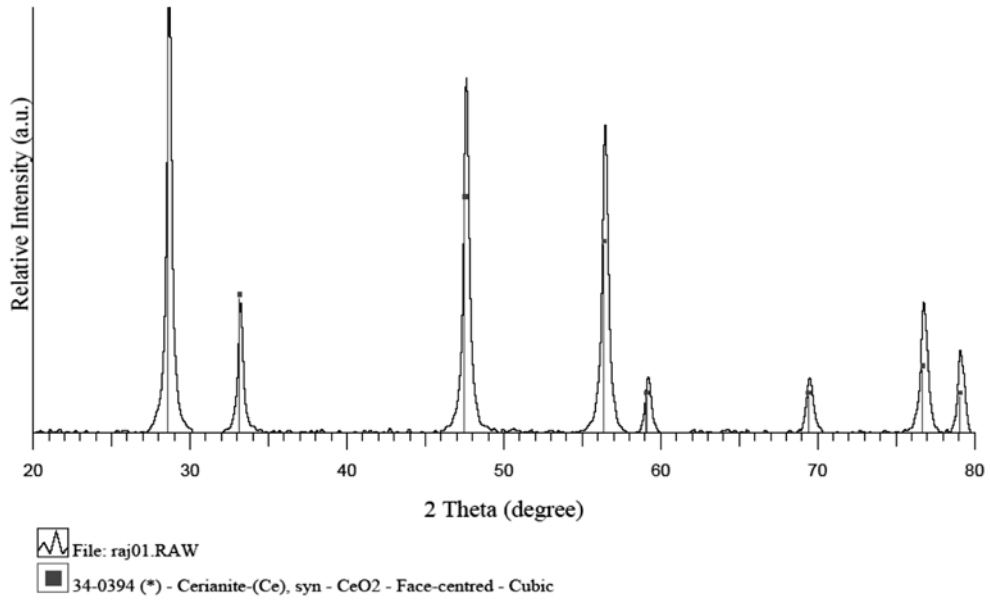

Fig. 7. XRD pattern of pure CeO_2.

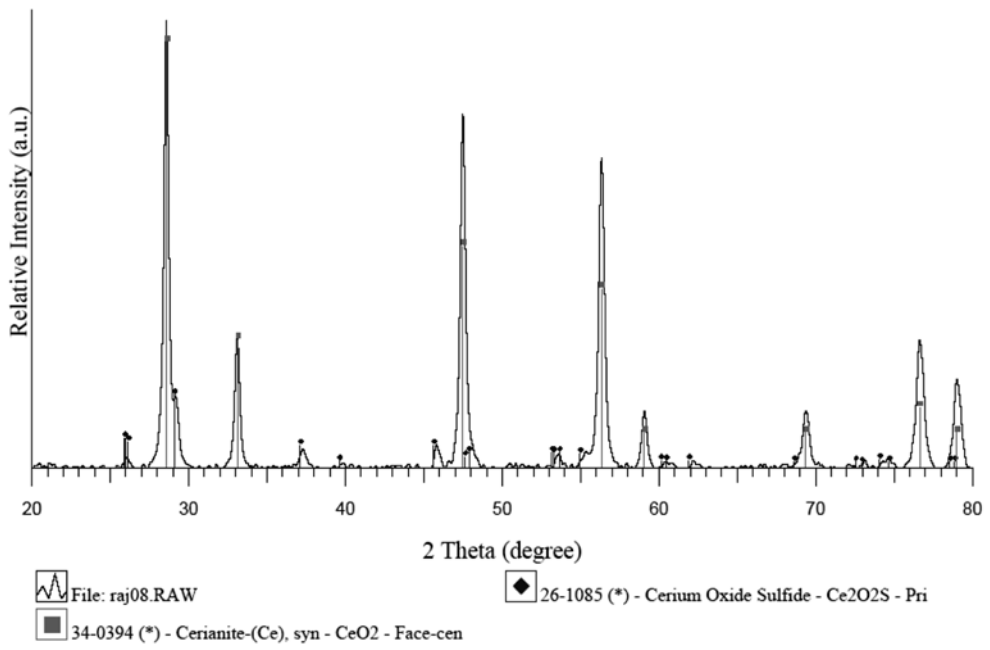

Fig. 8. XRD pattern of CeO_2 sulfided at 800 °C (JCPDS-ICDD).

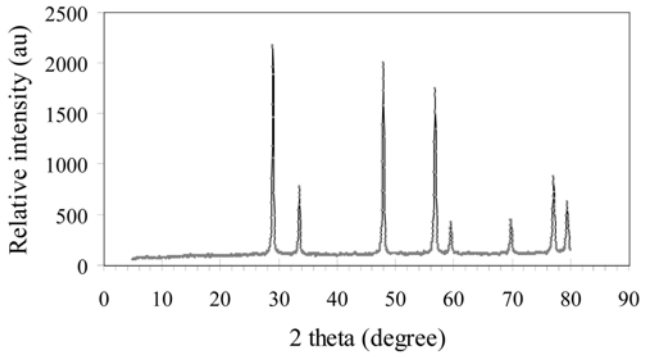

Fig. 9. XRD pattern of regenerated sulfided CeO_2 (JCPDS-ICDD).

CeO_2 peaks due to the formation of Ce_2O_2S. Sulfided CeO_2 was subjected to oxidative regeneration at a constant heating rate of 10 °C min^{-1} until 900 °C. The sample after regeneration was analyzed by XRD to determine its potential reuse as a CeO_2. It was found that the regenerated CeO_2 showed peaks at the same two theta angles as those of pure CeO_2 as shown in Fig. 9. This ensures the possible regeneration of sulfided CeO_2.

From the evidence of sulfidation, regeneration, and catalyst characterization, a sequence of reactions that occurred during these processes can be proposed. The possible reaction mechanism of the sulfidation and regeneration can be predicted as follows:

$$2CeO_2+H_2S \rightarrow Ce_2O_2S+H_2O+0.5O_2 \quad (4)$$

$$Ce_2O_2S+2O_2 \rightarrow SO_2+2CeO_2 \quad (5)$$

It should be noted that the detectable of steam from the desulfurization experiments and the observation of Ce_2O_2S phase from the XRD studies support this proposed sulfidation reaction mechanism: TPO and XRD analysis. The first experiment observed the formation of SO_2 from the regeneration process, while the second one confirmed that CeO_2 can be regenerated.

4. Deactivation Model for CeO_2 Absorbent

Deactivation models proposed in the literature [24] for gas-solid reactions with significant changes of activity of the solid due to textural changes, as well as product layer diffusion resistance during reaction, were reported to be quite successful in predicting conversion-time data. In the early work of Orbey et al. [16] and in the recent work of Suyadal et al. [25], deactivation models were used for the prediction of breakthrough curves in packed adsorption columns. In the present work, a deactivation model is proposed with the following assumptions: isothermal condition, pseudo-steady-state condition, first-order deactivation of the absorbent with respect to the solid surface which can be described in terms of an exponential decrease with time in its available surface, and constant activity throughout the surface of absorbent. The combined equation of mole balance and rate law for the packed bed reactor is given below:

$$Vo \cdot t\frac{dC_{H_2S}}{dt} = -k_o \cdot a(t) C_{H_2S} \quad (6)$$

The boundary conditions at inlet concentrations are

At t=0, $C_{H_2S}=C_{H_2Sin}$

At t=t, $C_{H_2S}=C_{H_2Sout}$

Therefore,

$$a(t)=\frac{Vo}{Wk}Ln\left(\frac{C_{H_2Sin}}{C_{H_2Sout}}\right) \quad (7)$$

The first order exponential decay is $a(t)=e^{-k_d t}$, substituting Eq. (6) to Eq. (8):

$$-k_d \cdot t = \ln\frac{Vo}{Wk_o} + \ln\ln\left(\frac{C_{H_2Sin}}{C_{H_2Sout}}\right) \quad (8)$$

This equation is equivalent to the breakthrough [25]. Thus, when $\ln\ln(C_{H_2Sin}/C_{H_2Sout})$ is plotted versus operating time (t), a straight line should be obtained with a slope equal to $-k_d$ and intercept equal to $\ln(Vo/Wk_o)$ as shown in Fig. 10. Table 3 summarizes the model parameters determined at different temperatures. The fluctuation of 10 to 15% in correlation coefficient may be due to initial bumps.

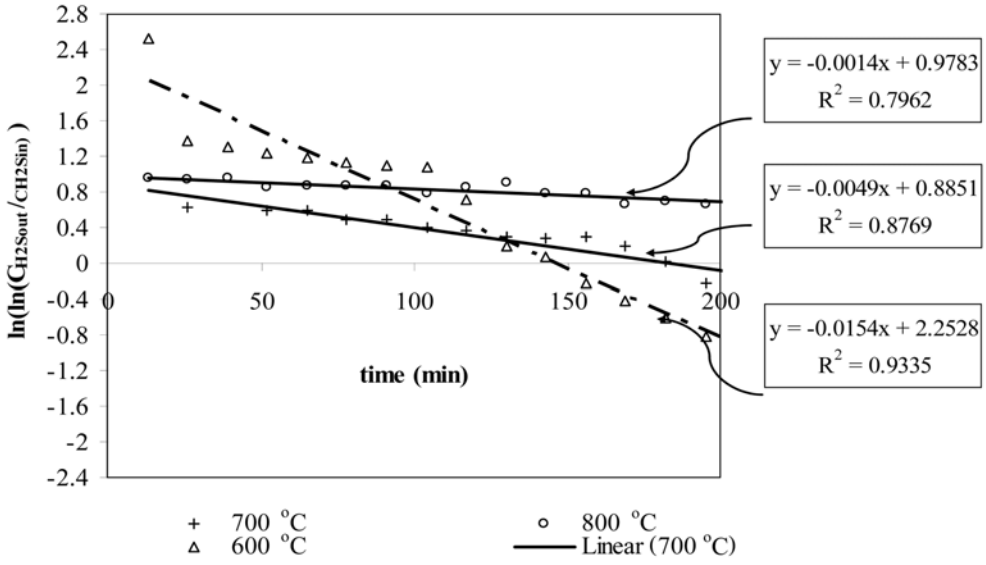

Fig. 10. Test of deactivation model equation.

Table 3. Summary of deactivation model parameters

Temperature (°C)	Vo/Wk$_o$ (-)	k$_o$ (cm^3 min^{-1} g^{-1})	k$_d$ (min^{-1})	R^2 (-)
600	2.55	3.566	0.0144	0.79
700	2.40	1.66	0.0049	0.89
800	2.66	1.503	0.0014	0.9351

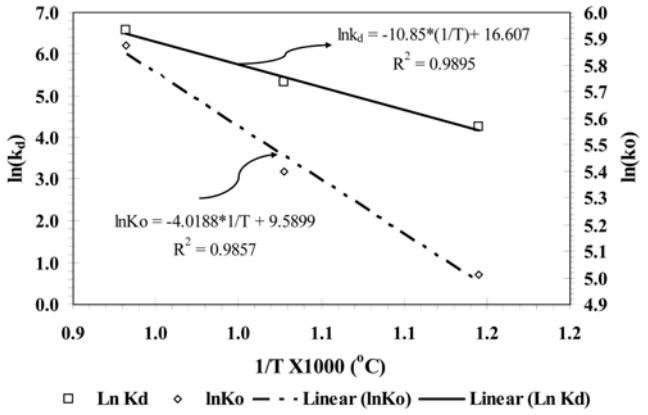

Fig. 11. Arrhenius plots of sorption rate constants and deactivation rate constants.

The advantage of the deactivation model is the presence of only two adjustable parameters such as initial sorption rate constant K_o and the deactivation rate constant K_d. Both parameters showed an increasing trend with respect to an increase in the temperature. Sorption rate constant K_o and the deactivation rate constant K_d were correlated as a function of temperature using by Arrhenius equations (Eqs. (9) and (10)).

$$K_o = k_o e^{-e/RT} \quad (9)$$

$$K_d = k_o e^{-e/RT} \quad (10)$$

The temeprature dependency was illustrated as shown in Fig. 11. The activation energies of k_o and k_d were found to be 33.4 and 90 kJ mol^{-1}. These high values of the activation energies indicate that the H_2S sorption on CeO_2 is chemical adsorption.

CONCLUSION

Nano-scale high surface area CeO_2 has useful desulfurization activity between 500 and 850 °C. Compared to the conventional low surface area CeO_2, 80-85% of H_2S was removed by nano-scale high surface area CeO_2, whereas 30-32% of H_2S was removed by conventional low surface area CeO_2. According to the XRD and EDS mapping, uniform Ce_2O_2S was formed after desulfurization. According to the TPO experiment, this component (Ce_2O_2S) can be recovered to CeO_2 after exposure in the oxidation condition at temperature above 600 °C. Furthermore, regarding the SEM/EDS and XRD measurements, all Ce_2O_2S forming is converted to CeO_2 after this oxidative regeneration.

As the final step, a deactivation model considering the concentration and temperature dependencies of the desulfurization activity was proposed for later application in the SOFC model.

ACKNOWLEDGMENT

The financial support from the Thailand Research Fund (TRF) and the Joint Graduate School of Energy and Environment (JGSEE) throughout this project is gratefully acknowledged. The authors are also thankful to Dr.Nakorn Srisukhumbowornchai for his valuable suggestions on XRD patterns.

REFERENCES

1. D. W. Park, B. H. Hwang, W. D. Ju, M. I. Kim, K. H. Kim and H. C. Woo, *Korean J. Chem. Eng.*, **22**, 190 (2005).
2. J. D. Lee, J. H. Jun, N. K. Park, S. O. Ryu and T. J. Lee, *Korean J. Chem. Eng.*, **22**, 36 (2005).
3. P. R. Westmoreland and D. P. Harrison, *Environ. Sci. Technol.*, **10**, 559 (1976).
4. H. T. Jang, S. B. Kim and D. S. Doh, *Korean J. Chem. Eng.*, **20**, 116 (2003).
5. T. H. Gardener, *Fuel*, **81**, 2157 (2002).
6. J. H. Swisher and K. Schwerdtfeger, *J. Mater. Eng. Perform.*, **1**, 399 (1992).
7. V. Patrick and G. R. Gavalas, *Ind. Eng. Chem. Res.*, **28**, 931 (1989).
8. V. V. Meng and D. A. R. Kay, *High technology ceramics*, Elsevier, Amsterdam, 2247 (1987).
9. D. A. R. Kay, W. G. Wilson and V. Jalan, *J. Alloys and Compounds*, **192**, 11 (1993).
10. K. H. Kim, S. Y. Lee and K. J. Yoon, *Korean J. Chem. Eng.*, **23**, 356 (2006).
11. K. H. Kim, S. Y. Lee, S. W. Nam, T. H. Lim, S. A. Hong and K. J. Yoon, *Korean J. Chem. Eng.*, **23**, 17 (2006).
12. J. Abbasian, A. H. Hill, M. Flytzani-Stephanopoulos and Z. Li, Final Report, DE-FC22-92PC92521 (1994).
13. Z. Li and M. Flytzani-Stephanopoulos, *Ind. Eng. Chem. Res.*, **36**, 187 (1997).
14. Y. Zeng, S. Zhang, F. R. Groves and D. P. Harrison, *Chem. Eng. Sci.*, **54**, 3007 (1999).
15. N. Laosiripojana and S. Assabumrungrat, *Applied Catal. B*, **60**, 107 (2005).
16. N. Orbey, G. Dogu and T. Dogu, *Can. J. Chem. Eng.*, **60**, 314 (1982).
17. H. S. Fogler, *Elements of chemical reaction engineering*, Prentice-Hall Inc, Englewood Cliffs, New Jersey 07632, ISBN 0-13-263476-7 (1986).
18. M. P. Cal, B. W. Strickler and A. A. Lizzio, *Carbon*, **38**, 1757 (2000).
19. R. M. Ferriz, R. J. Gorte and J. M. Vohs, *Applied Catal. B*, **43**, 273 (2003).
20. Z. Wang and M. Flytzani-Stephanopoulos, *Energy & Fuels*, **19**, 2093 (2005).
21. M. Flytzani-Stephanopoulos, Angela D. Surgenor, Report, NASA/TM-2007-214686.
22. S. Yasyerli, G. Dogu and T. Dogu, *Catal. Today*, **117**, 271 (2006).
23. M. Ziolek, *J. Molecular Catalysis A*, **97**, 49 (1995).
24. T. Dogu, *Chem. Eng. J.*, **21**, 213 (1981).
25. Y. Suyadal, M. Erol and H. Oguz, *Ind. Eng. Chem. Res.*, **39**, 724 (2000).